

Koopman analysis of the periodic Korteweg-de Vries equation

Jeremy P Parker^{1, a)} and Claire Valva²

¹⁾*Emergent Complexity in Physical Systems Laboratory (ECPS), École Polytechnique Fédérale de Lausanne, Lausanne, Switzerland*

²⁾*Courant Institute of Mathematical Sciences, New York University, New York, New York, USA*

The eigenspectrum of the Koopman operator enables the decomposition of nonlinear dynamics into a sum of nonlinear functions of the state space with purely exponential and sinusoidal time dependence. For a limited number of dynamical systems, it is possible to find these Koopman eigenfunctions exactly and analytically. Here, this is done for the Korteweg-de Vries equation on a periodic interval, using the periodic inverse scattering transform and some concepts of algebraic geometry. To the authors' knowledge, this is the first complete Koopman analysis of a partial differential equation which does not have a trivial global attractor. The results are shown to match the frequencies computed by the data-driven method of dynamic mode decomposition (DMD). We demonstrate that in general DMD gives a large number of eigenvalues near the imaginary axis, and show how these should be interpreted in this setting.

Dynamic mode decomposition (DMD) is a widely used computational method for analysing spatiotemporal data from experiments, observations and numerics. The connection to the mathematical Koopman operator means that we can understand the behaviour of DMD by analytically applying the Koopman operator to integrable partial differential equations. One non-trivial example is the Korteweg-de Vries equation on a periodic domain, which admits both wavelike and soliton solutions, and can be solved analytically via the inverse scattering method.

I. INTRODUCTION

The Koopman operator was introduced by Koopman¹ to describe the nonlinear behaviour of a dynamical system as the linear evolution of nonlinear observables of that system. It is well known that a finite dimensional nonlinear system can be converted into an infinite dimensional linear system; Koopman analysis extends this to infinite dimensional nonlinear systems. Recent interest in the Koopman operator was initiated by Igor Mezić^{2,3}, and it has become popular for its close connection to the computational method of dynamic mode decomposition.

DMD was originally invented by Schmid⁴ as a method for simultaneously extracting the important spatial and temporal features of a timeseries. It has been successfully applied to a wide array of numerical, observational and experimental data, most notably in fluid dynamics⁵⁻⁷. Under certain conditions⁸, the results of DMD can be seen as a numerical approximation to the Koopman modes and eigenvalues of the underlying dynamical system, and so understanding the Koopman operator aids

interpretation of the results of DMD. In particular, to understand the spatial patterns called DMD modes, it would be helpful to have analytic results on nonlinear partial differential equations (PDEs).

Several authors⁹⁻¹¹ have successfully performed Koopman analysis on the Burgers equation, a dissipative nonlinear PDE which can be transformed into the linear heat equation with a suitable change of variables. Nakao and Mezić¹² considered the Burgers equation as well as a non-trivial transformation of it to the phase-diffusion equation. Though insightful, these PDEs admit only a single steady global attractor, and are strongly dissipative, which precludes a lot of interesting nonlinear behaviour relevant to applying DMD to situations involving sustained waves, a common use-case.

Parker and Page¹³ considered the Korteweg-de Vries (KdV) equation, an integrable partial differential equation of one variable. This Hamiltonian dynamical system behaves very differently from the dissipative systems mentioned above. In that work, some Koopman eigenfunctions were found for soliton solutions of the KdV equation on the real line which excluded a large class of solutions; in particular, this excluded the spatially periodic solutions which are the natural choice for computer simulations of solitons. It was argued that the simplest periodic solutions, cnoidal waves, give purely imaginary Koopman eigenvalues, in sharp contrast to the isolated solitons, which have purely real Koopman eigenvalues, despite being a naturally limiting case of the former.

A periodic domain is the natural setting for numerical solutions of 1-dimensional PDEs like the KdV equation. Indeed, early pioneering numerical simulations of the KdV equation on a periodic domain¹⁴ were used to shed light on the famous Fermi-Pasta-Ulam-Tsingou problem¹⁵, in which the initial state of a system recurs to arbitrary precision after complex nonlinear dynamics. It was later proven¹⁶ that this is because the solutions lie on quasi-periodic invariant tori. We will show that it is possible to use DMD to determine the underlying frequencies. In fact, when the dynamics are confined to an invariant torus, DMD is equivalent to a Fourier transform

^{a)}Author to whom correspondence should be addressed: jeremy.parker@epfl.ch

in time, though it generalises when other modes grow or decay.

In the present paper, we study a particular but very general class of solutions of the KdV equation on a periodic interval, for which we are able to define Koopman eigenfunctions. These eigenfunctions require the evaluation of contour integrals on Riemann surfaces which must be performed numerically in all but the simplest of cases. This method is not, therefore, recommended as a general approach for nonlinear PDEs, where DMD could easily be applied. However, the semi-formal mathematical treatment presented here gives instructive results: we will see that in this case, Koopman eigenvalues necessary for the decomposition of the state of the system densely fill the imaginary axis, and so the results of DMD are subtle to interpret. The paper proceeds as follows: in section II the KdV equation is introduced and its history and significance briefly described; in section III the Koopman operator and its spectrum are defined; in section IV we then derive Koopman eigenfunctions for the KdV equation; section V presents the results of applying these to an example solution, which is compared to the numerical results of DMD in section VI. Concluding remarks are given in section VII.

II. THE KDV EQUATION

The KdV equation¹

$$\begin{aligned} 4\partial_t u(x, t) &= 6u(x, t) \partial_x u(x, t) + \partial_x^3 u(x, t), \\ u(x, 0) &= u_0(x), \end{aligned} \quad (1)$$

was derived by Korteweg and de Vries¹⁸ to describe the weakly nonlinear evolution of shallow water waves propagating in one direction. The pioneering computational results of Zabusky and Kruskal¹⁴ demonstrated the existence of soliton solutions when this equation is solved on a finite periodic domain. For an infinite domain, the celebrated inverse scattering method of Gardner et al.¹⁹ gives a straightforward procedure to solve the equation, and provides intuitive interpretations for the existence of solitons as conserved quantities. Analytical results on a periodic interval have proven much more complicated, despite the early computation successes and the well known cnoidal wave solution.

In addition to shallow water waves, the KdV equation naturally arises from weakly nonlinear theory in many physically relevant flows^{20–22}. Our interest however derives from the fact that the equation admits complex, nonlinear but non-chaotic solutions amenable to analytic treatment. Unlike other PDEs for which Koopman spectra have been derived, it is a Hamiltonian system with

an infinite number of conserved quantities, rather than having one unique attractor.

The solution to (1) is well-posed on $\mathbb{T} = \mathbb{R}/2\pi\mathbb{Z}$, the periodic domain of length 2π , for initial conditions in Sobolev spaces $H^s(\mathbb{T}, \mathbb{R})$ with $s \geq -1$ ²³, with a well-defined evolution operator $\mathcal{S}_t : H^s(\mathbb{T}, \mathbb{R}) \rightarrow H^s(\mathbb{T}, \mathbb{R})$ for each time t . A single periodic wave of sufficient amplitude breaks down into a spatially periodic solution, with quasi-periodic behaviour in time. That is to say, solutions lie on an invariant torus, as is usual for integrable Hamiltonian systems, and these invariant tori foliate phase space. In fact, any solution of (1) can be approximated to arbitrary precision as an invariant M -torus¹⁶, $M \in \mathbb{N}$. These are the so-called ‘finite gap’ solutions, which will be the focus of the present study. Practically, the evolution of an arbitrary initial condition can be approximated by truncating the scattering data at a judiciously chosen M ²⁴.

Let us therefore define our solution space Ω_M to be the subset of $L^2(\mathbb{T}, \mathbb{R})$ for which there are M -gap solutions (this terminology should become clearer in section IV). This is a well-posed invariant subspace. For convergent Koopman decompositions it will be necessary to further restrict this space, in a manner analogous to that of Balabane et al.¹¹, in section V.

It will be useful later to make the so-called Hirota transformation $u \mapsto \vartheta$ defined by²⁵

$$u(x, t) = 2\partial_x^2 \log \vartheta(x, t), \quad (2)$$

so that (1) becomes

$$4\vartheta \partial_x \partial_t \vartheta - 4\partial_x \vartheta \partial_t \vartheta - 3(\partial_x^2 \vartheta)^2 + 4\partial_x \vartheta \partial_x^3 \vartheta - \vartheta \partial_x^4 \vartheta = 0. \quad (3)$$

This is analogous to the Cole-Hopf transformation exploited by previous authors for the Burgers equation^{9–11}, though in this case the transformation seems at first glance to have made the equation more complicated. The utility comes from the fact that ϑ can be expressed as a Riemann theta function, as explained in section IV.

III. THE KOOPMAN OPERATOR

Let \mathcal{O}_M be the space of continuous maps $\Omega_M \rightarrow \mathbb{C}$, which are called observables of the system. The Koopman operator, a composition operator for dynamical systems, is defined for each $t \geq 0$ by

$$\begin{aligned} \mathcal{K}_M^t : \mathcal{O}_M &\rightarrow \mathcal{O}_M, \\ [\mathcal{K}_M^t \phi] (u_0) &= \phi(u(\cdot, t)), \end{aligned} \quad (4)$$

for any observable $\phi \in \mathcal{O}_M$, where the evolution of $u(x, t)$ is governed by (1). The Koopman operator is a linear operator, amenable to spectral theory. The *Koopman eigenvalues* $\lambda \in \mathbb{C}$ and *Koopman eigenfunctions* $\varphi \in \mathcal{O}_M$ satisfy

$$[\mathcal{K}_M^t \varphi] (u_0) = e^{\lambda t} \varphi(u_0) \quad (5)$$

¹ Many different conventions are employed in the literature, and notably solitons can be either positive or negative depending on this choice. Here we follow Belokolos et al.¹⁷.

or equivalently

$$\varphi(u(\cdot, t)) = e^{\lambda t} \varphi(u_0). \quad (6)$$

A simple example of a Koopman eigenfunction would be any conserved quantity of the dynamics, with eigenvalue $\lambda = 0$. More generally, they are any observable for which the temporal behaviour is purely (complex) exponential as the state evolves. Since the system we study is Hamiltonian, we expect only purely imaginary eigenvalues $\lambda = i\omega$, giving purely oscillatory behaviour. In certain circumstances, it may be possible that the Koopman eigenfunctions form a basis for \mathcal{O}_M , in which case we can decompose all other observables as a sum over Koopman eigenfunctions. In particular, we are interested in whether it is possible to write the state of the system u as a convergent sum

$$u(x, t) = \sum_{\nu} c_{\nu}(x) \varphi_{\nu}(u_0) e^{i\omega_{\nu} t}. \quad (7)$$

Here the $c_{\nu} : \mathbb{T} \rightarrow \mathbb{C}$ are called *Koopman modes*, which encode spatial information for each eigenvalue and are independent of the particular choice of initial condition u_0 , whose contribution is included in the value of $\varphi_{\nu}(u_0)$. If this is possible, it means that the dynamics of (1) can be decomposed as a sum over nonlinear functions whose temporal behaviour is purely oscillatory in time.

IV. KOOPMAN EIGENFUNCTIONS OF THE KDV EQUATION

It would take a whole textbook to fully explain the periodic inverse scattering transform. We refer readers to the textbooks by Novikov et al.²⁶, Belokolos et al.¹⁷ and Osborne²⁷ for accessible introductions, including the necessary background of Riemann surfaces and theta functions, though note the differing notations and conventions between these (we follow the notation of Belokolos et al.¹⁷). Here we give a summary of the relevant results for the KdV equation which are implemented in the Mathematica notebook given in the supplementary materials.

One of the key results in the solution of the KdV equation was the discovery of a Lax pair²⁸: a pair of linear operators $L(u), A(u) : L^2(\mathbb{R}) \rightarrow L^2(\mathbb{R})$ such that

$$\frac{dL}{dt} = L(t) \circ A(t) - A(t) \circ L(t), \quad (8)$$

where $L(t) := L(u(\cdot, t))$ etc. In the case of the KdV equation (1),

$$L(u) = -\frac{d^2}{dx^2} - u, \quad (9)$$

$$A(u) = \frac{d^3}{dx^3} + \frac{3}{4} \left(u \frac{d}{dx} + \frac{d}{dx} u \right). \quad (10)$$

The operator (10) is skew-adjoint. The operator (9) is the well known self-adjoint Schrödinger operator, with

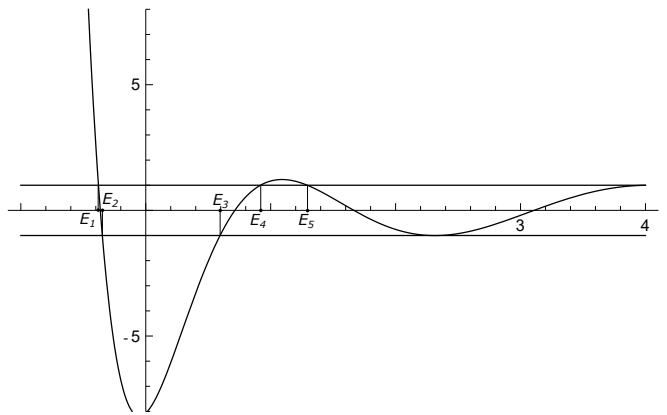


FIG. 1. $F(\lambda)$, half the trace of the monodromy matrix, against real λ , for $u_0(x) = \sin x$. Allowable values of λ for a bounded eigenfunction are when $|F(\lambda)| \leq 1$. The forbidden regions $(-\infty, E_1)$, (E_2, E_3) , \dots are called gaps.

potential u . From (8) it can be shown that the spectrum of L is independent of t , when $u(x, t)$ satisfies (1). Finding eigenvalues $\lambda \in \mathbb{R}$ and eigenfunctions $\psi \in C^\infty$ reduces to the Sturm-Liouville problem

$$\psi'' + u\psi + \lambda\psi = 0. \quad (11)$$

In the case of a periodic potential $u(x+2\pi) = u(x)$, equation (9) is known as Hill's operator and has been widely studied²⁹. The admissible eigenvalues λ for a bounded eigenfunction ψ reside in intervals $[E_1, E_2]$, $[E_3, E_4]$, \dots , where $-\infty < E_1 < E_2 \leq E_3 < E_4 \leq E_5 < \dots$. Outside these regions, only unbounded solutions are possible, and these are termed forbidden gaps. The E_k are the values of λ for which $F(\lambda)$, defined as half the trace of the monodromy matrix of (11), is ± 1 ²⁹ (see figure 1). Though the monodromy matrix is not invariant under the dynamics (1), its trace, and therefore also the E_k , are invariant. We explicitly consider only the case when there is a finite number g of non-degenerate forbidden gaps (E_2, E_3) , (E_4, E_5) , \dots , so that $E_{2k} = E_{2k+1}$ for all $k > g$.

The hyperelliptic curve

$$\mu^2 = \prod_{j=1}^{2g+1} (\lambda - E_j) \quad (12)$$

defines a Riemann surface of two sheets, with a branch point at each E_j (see figure 2). The *genus* of this surface is simply the number of gaps g . It is then possible to define a basis of contours a_j and b_j ($1 \leq j \leq g$) for the Riemann surface such that any contour can be expressed, up to continuous deformations, as a sum of the a_j and b_j . Such a choice of basis is not unique, and will have implications for the final results – see discussions of the wave basis and soliton basis in Osborne²⁷. Our convention is shown in figure 3. We also define a basis of holomorphic differentials on this surface

$$\tilde{\omega}_k = \frac{\lambda^{g-k} d\lambda}{\mu} \quad (13)$$

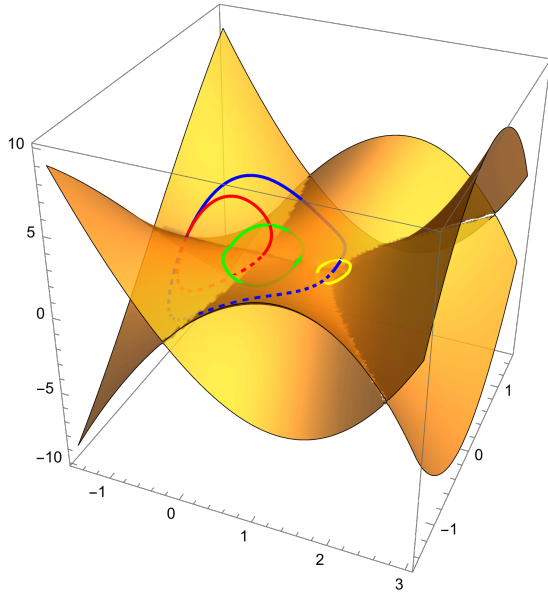


FIG. 2. Riemann surface of genus 2 for the initial condition $u_0(x) = \sin x$, truncated to a 2-gap solution. The horizontal axes show the real and imaginary parts of λ and the vertical axis shows the real part of μ , as defined by (12).

and then make a linear transformation to the canonical basis $\omega_k = \sum_j \mathbf{c}_{kj} \hat{\omega}_j$ such that

$$\int_{a_j} \omega_k = 2\pi i \delta_{jk}, \quad j, k = 1, \dots, g. \quad (14)$$

In this new basis, we define the *period matrix* of the Riemann surface

$$\mathbf{B}_{jk} = \int_{b_j} \omega_k. \quad (15)$$

It can be shown that this matrix is symmetric $\mathbf{B}_{jk} = \mathbf{B}_{kj}$ with all entries having strictly negative real part. It is then the case that the transformed variable ϑ can be written as

$$\vartheta(x, t) = \theta(\mathbf{U}x + \mathbf{W}t + \mathbf{D}, \mathbf{B}) \quad (16)$$

where we define the Riemann theta function

$$\theta(\mathbf{z}, \mathbf{B}) = \sum_{\mathbf{m} \in \mathbb{Z}^g} \exp\left(\frac{1}{2} \mathbf{m}^T \mathbf{B} \mathbf{m} + \mathbf{z}^T \mathbf{m}\right). \quad (17)$$

For \mathbf{B} real and \mathbf{z} imaginary, this gives real values by symmetry. The wavenumber vector \mathbf{U} and frequency vector \mathbf{W} are calculated as

$$\mathbf{U}_j = 2i \mathbf{c}_{j1}, \quad (18)$$

$$\mathbf{W}_j = -2i \left(\mathbf{c}_{j2} + \frac{1}{2} \mathbf{c}_{j1} \sum_{k=1}^{2g+1} E_k \right). \quad (19)$$

By construction, the \mathbf{U}_j must be integers, but the frequencies \mathbf{W}_j will be incommensurate in general. Both \mathbf{U}

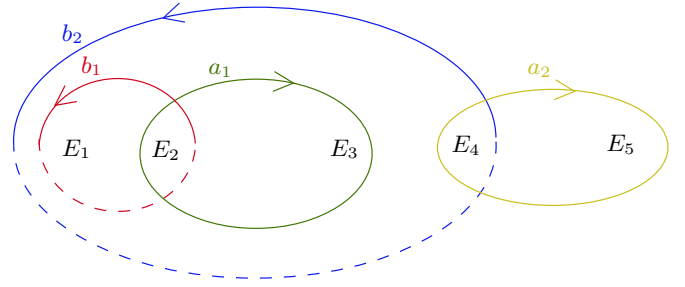


FIG. 3. Schematic of the basis of contours for a $g = 2$ Riemann surface, where dashed lines show the parts of the contour taken on the second sheet. The colours are as for figure 2.

and \mathbf{W} are purely imaginary. Since they are calculated only from the E_k , all of \mathbf{B} , \mathbf{U} and \mathbf{W} are constant as the system evolves. The value of the vector of phases \mathbf{D} , conversely, depends on the particular state at time $t = 0$ (and its evolution is absorbed into \mathbf{W}).

To find the phases \mathbf{D} , it is necessary to define a second set of eigenvalues for the Sturm-Liouville problem (11), now with the boundary conditions $\psi(0) = \psi(2\pi) = 0$. This discrete set of eigenvalues $\lambda_1, \lambda_2, \dots$ lies in the gaps so that $E_2 < \lambda_1 < E_3$, $E_4 < \lambda_2 < E_5$ etc. These eigenvalues are not constant as the state evolves, and depend on the time of measurement. The formula for \mathbf{D} is then given by¹⁷

$$\mathbf{D}_j = - \sum_{k=1}^g \int_{-\infty}^{\lambda_k} \omega_j - \sum_{k=1}^g \mathbf{B}_{jk} + i\pi j, \quad (20)$$

where here λ_k represents a point on the surface with $\lambda = \lambda_k$, with care be taken to evaluate the integral on the correct sheet. \mathbf{D} is also purely imaginary.

Finally, this allows us to define a Koopman eigenfunction for (1) for each $\mathbf{m} \in \mathbb{Z}^g$:

$$\varphi_{\mathbf{m}}(u_0) := \exp(\mathbf{D}^T \mathbf{m}) \quad (21)$$

which then evolves as

$$\varphi_{\mathbf{m}}(u(\cdot, t)) = \exp(\mathbf{W}^T \mathbf{m} t) \exp(\mathbf{D}^T \mathbf{m})$$

and thus has Koopman eigenvalue $\mathbf{W}^T \mathbf{m}$, an integer linear combination of the fundamental frequencies. As the frequencies are incommensurate, for genus $g = 2$ and greater, these eigenvalues densely fill the imaginary axis. This is a significant complication over previously studied PDEs. Note that $\varphi_{\mathbf{m}_1}(u) \varphi_{\mathbf{m}_2}(u) = \varphi_{\mathbf{m}_1 + \mathbf{m}_2}(u)$, and $\varphi_{\mathbf{0}}(u) = 1$.

V. KOOPMAN DECOMPOSITIONS

Clearly the expression (16) is directly a convergent Koopman decomposition for $\vartheta(x, t)$, as it is a sum of

terms whose time dependence is purely exponential. We can write it as

$$\vartheta(x, 0) = \sum_{\mathbf{m} \in \mathbb{Z}^g} e^{U^T \mathbf{m} x} \exp\left(\frac{1}{2} \mathbf{m}^T \mathbf{B} \mathbf{m}\right) \varphi_{\mathbf{m}}(u_0). \quad (22)$$

It is somewhat more involved to obtain a decomposition of u , but this is still possible so long as ϑ is sufficiently small, via (2):

$$\begin{aligned} u_0(x) &= 2\partial_x^2 \log \left[1 + \sum_{\mathbf{m} \in \mathbb{Z}^g \setminus \{\mathbf{0}\}} \exp\left(\frac{1}{2} \mathbf{m}^T \mathbf{B} \mathbf{m} + U^T \mathbf{m} x\right) \varphi_{\mathbf{m}}(u_0) \right] \\ &= -2\partial_x^2 \left[\sum_{n=1}^{\infty} \frac{(-1)^n}{n} \sum_{\mathbf{m}_1, \dots, \mathbf{m}_n \in \mathbb{Z}^g \setminus \{\mathbf{0}\}} \exp\left\{ \sum_{q=1}^n \left(\frac{1}{2} \mathbf{m}_q^T \mathbf{B} \mathbf{m}_q + U^T \mathbf{m}_q x \right) \right\} \prod_{q=1}^n \varphi_{\mathbf{m}_q}(u_0) \right] \\ &= \sum_{\mathbf{m} \in \mathbb{Z}^g} \left(-2 (U^T \mathbf{m})^2 e^{U^T \mathbf{m} x} \sum_{n=1}^{\infty} \frac{(-1)^n}{n} \sum_{\substack{\mathbf{m}_1, \dots, \mathbf{m}_n \in \mathbb{Z}^g \setminus \{\mathbf{0}\} \\ \sum_q \mathbf{m}_q = \mathbf{m}}} \exp\left\{ \sum_{q=1}^n \frac{1}{2} \mathbf{m}_q^T \mathbf{B} \mathbf{m}_q \right\} \right) \varphi_{\mathbf{m}}(u_0). \end{aligned} \quad (23)$$

This complicated series is absolutely convergent when $0 < \vartheta(x, t) < 2$. For larger ϑ , other expansions could be found, using only the Koopman eigenfunctions given in the previous section. To summarise this expression, we

have found a Koopman decomposition for u using Koopman eigenfunctions $\varphi_{\mathbf{m}}(u_0)$ with Koopman eigenvalues $\mathbf{W}^T \mathbf{m}$. The corresponding Koopman modes are

$$-2 (U^T \mathbf{m})^2 e^{U^T \mathbf{m} x} \sum_{n=1}^{\infty} \frac{(-1)^n}{n} \sum_{\substack{\mathbf{m}_1, \dots, \mathbf{m}_n \in \mathbb{Z}^g \setminus \{\mathbf{0}\} \\ \sum_q \mathbf{m}_q = \mathbf{m}}} \exp\left\{ \sum_{q=1}^n \frac{1}{2} \mathbf{m}_q^T \mathbf{B} \mathbf{m}_q \right\} \quad (24)$$

Notice that these are purely sinusoidal in x . The Koopman modes depend on \mathbf{U} and \mathbf{B} , which are functions of the Riemann surface and therefore of the g -torus to which the dynamics are constrained in phase space, but the Koopman modes do not depend on the choice of initial conditions beyond this.

As a concrete example, we consider the initial condition $u_0(x) = \sin x$. Despite the simplicity of this choice, it gives an apparently infinite number of non-degenerate gaps (see figure 1), but using only $g = 2$ or $g = 3$ results in good agreement. With $g = 4$, not shown here, the reconstructed solution is virtually indistinguishable from the initial condition. Only two solitons are visible per spatial period in a numerical solution; the genus of the Riemann surface is not the number of solitons. For $g = 2$ we find numerically that

$$\mathbf{U} = (-1i, -2i), \quad \mathbf{W} \approx (-0.036, 1.930i), \quad (25)$$

$$\mathbf{B} \approx \begin{pmatrix} -3.171 & -1.930 \\ -1.930 & -7.247 \end{pmatrix}, \quad (26)$$

and for $g = 3$

$$\mathbf{U} = (-1i, -2i, -3i), \quad \mathbf{W} \approx (-0.036i, 1.931i, 6.741i), \quad (27)$$

$$\mathbf{B} \approx \begin{pmatrix} -3.171 & -1.929 & -1.321 \\ -1.929 & -7.247 & -3.190 \\ -1.321 & -3.190 & -12.810 \end{pmatrix}. \quad (28)$$

The reconstructed $u(x, t)$ given by a finite truncation of the Koopman decomposition (23) is shown in figures 4 and 5. Including terms higher than $n = 4$ in the series may increase the accuracy of these, but the Koopman modes become prohibitively expensive to evaluate numerically.

VI. DYNAMIC MODE DECOMPOSITION

Given a discrete time-series of snapshots $\{\mathbf{v}_j\}_j$ from some dynamical system, DMD seeks to find a linear map A such that $\mathbf{v}_{j+1} = A\mathbf{v}_j$. In practice, DMD finds an

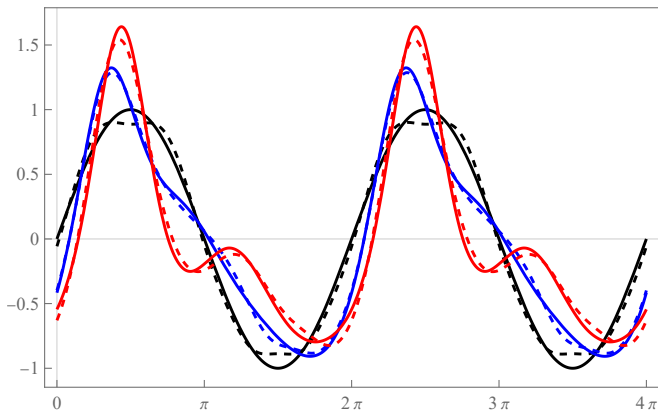


FIG. 4. Numerical solution u (solid) and Koopman reconstruction (dashed) at $t = 0$ (black), $t = 0.5$ (blue) and $t = 1$ (red) using $g = 2$, i.e. assuming the dynamics are constrained to a 2 dimensional quasiperiodic invariant torus. The Koopman decomposition (23) is truncated after $n = 4$ with $\mathbf{m}, \mathbf{m}_q \in \{-3, \dots, 3\}^2 \setminus \mathbf{0}$.

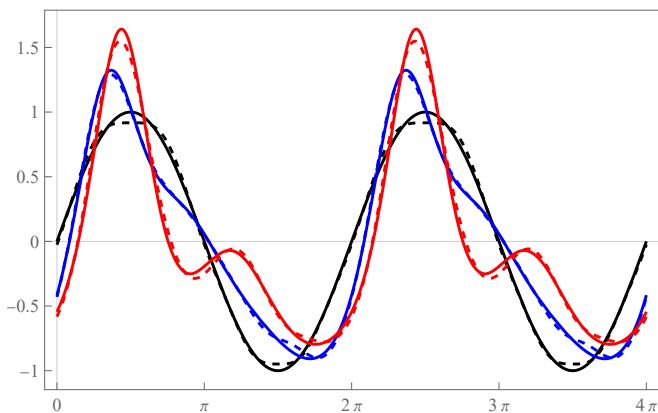


FIG. 5. As for figure 4 but with $g = 3$, and $\mathbf{m}, \mathbf{m}_q \in \{-3, \dots, 3\}^3 \setminus \mathbf{0}$.

eigendecomposition of A in which each mode of the decomposition has an associated amplitude a_k , spatial pattern \mathbf{u}_k and growth rate λ_k . As in the case of the Koopman eigenvalues, we expect $\lambda_k = i\omega_k$ to be purely imaginary because the system is Hamiltonian. We can use our expectation of purely imaginary eigenvalues as a heuristic for a well-resolved mode: if $|\text{Re}(\lambda_k)| \gg 0$ we infer that ω_k is an inaccurate guess. Then if the time between snapshots is τ , we can reconstruct the evolution of the system as

$$\mathbf{v}_j = \sum_k e^{i\omega_k j \tau} \mathbf{u}_k.$$

In the original and most basic form of the algorithm, the number of DMD modes that come from the spectral decomposition will be equal to the spatial dimension. We can increase both the robustness and number of discovered DMD modes found with delay embedding, a higher-order extension in which temporal resolution is

substituted for spatial resolution⁷. We found much better results when employing delay embedding; we used 20 delays.

As DMD is designed to detect the important temporal frequencies of the dynamics, it should be possible to use it to reconstruct an approximation $\tilde{\mathbf{W}}$ for \mathbf{W} from a time-series. However, as discussed in section IV, the Koopman eigenvalues densely fill the imaginary axis, and so the results of DMD are obscured. For example, if we expect the solution to be well-represented by an invariant 2-torus — and the DMD eigenfrequencies ω_k are sufficiently well-resolved — we expect to see $i\omega_k = n_{1k}\mathbf{W}_1 + n_{2k}\mathbf{W}_2$, for many different $n_{1k}, n_{2k} \in \mathbb{Z}$. However, as hinted at in section V, the amplitudes associated with low n_{jk} should be larger. Aided by knowing the relative amplitude of each DMD mode (to empirically identify “important” modes), we can guess the smaller of the $\tilde{\mathbf{W}}_j$ to be the gap between eigenvalues (and the smaller high amplitude mode) and the larger $\tilde{\mathbf{W}}_j$ to be the second largest high amplitude mode. We can extend this argument in the obvious way for $g > 2$.

We apply DMD to a numerical solution of (1) with initial condition $u_0(x) = \sin x$ as in section V. Our numerical simulation has a length of 450 time units, with a time resolution $\tau = 0.1$. We find very good agreement in the identification of \mathbf{W} as computed analytically to those found in DMD:

$$\tilde{\mathbf{W}} \approx (0.036i, 1.931i, 6.739i). \quad (29)$$

Note that the differing signs represent a degeneracy of the formulation, these could be recovered in the analytic method by using a different basis of integration contours. Figure 6 shows the DMD eigenvalues as well as their relative amplitudes.

Additionally, given that we know the Riemann theta function form (17), we can exploit the Hirota transform (2). By applying DMD to a time-series of ϑ rather than u , we can recover all parameters for the Riemann theta function, i.e. \mathbf{U} , \mathbf{W} and \mathbf{B} . The details of this procedure are given in the appendix. We find

$$\tilde{\mathbf{B}} \approx \begin{pmatrix} -3.077 & -1.907 \\ -1.907 & -7.150 \end{pmatrix} \quad (30)$$

which is approximately consistent with the values computed analytically, given in (28).

VII. DISCUSSION

We have performed a Koopman decomposition of the periodic KdV equation. This is almost immediate once the convoluted but well-defined process of periodic inverse scattering is performed. Additionally, we have shown how this result relates to the output of DMD for such a system. DMD gives a very large number of near-imaginary eigenvalues associated with the different harmonics of the nonlinearly interacting waves, which cor-

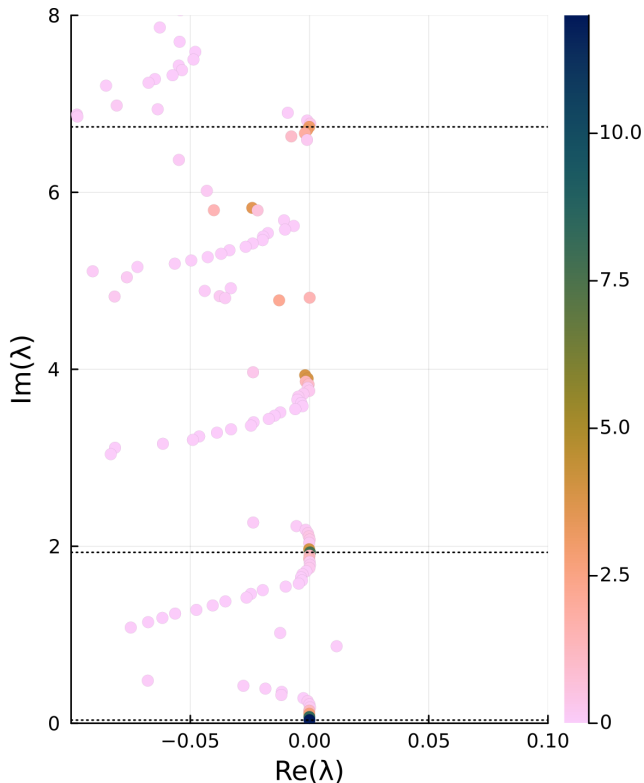


FIG. 6. DMD eigenvalues λ from analysis of a timeseries of u , where points are coloured to represent the amplitude ($|a|$) of each DMD mode (the colorbar saturates at 10). We plot only eigenvalues with real part less than 0.1 in magnitude, which excludes a number of spurious modes. Horizontal lines at $\tilde{\mathbf{W}}_1 = 0.03558i$, $\tilde{\mathbf{W}}_2 = 1.9312i$, and $\tilde{\mathbf{W}}_3 = 6.7394i$ mark the DMD approximations of \mathbf{W} . Prominent eigenvalues are also evident near $2\mathbf{W}_1$, $2\mathbf{W}_2$, $\mathbf{W}_1 + \mathbf{W}_2$, $\mathbf{W}_3 - \mathbf{W}_2$, etc.

respond to the Koopman eigenvalues found analytically, which densely fill the imaginary axis.

Further, by exploiting the θ -function representation of the solution, we are able to use DMD to approximately recover the necessary parameters.

We note in passing that since we expect purely imaginary eigenvalues in our system, it is a potential use-case for the physics-informed DMD method³⁰ of finding a unitary matrix A to fit the data. However, we found that this obfuscates the results, as it prevents the use of the real part of the eigenvalue as a measure for how well-resolved a given mode is.

The analytic results of this paper could be extended to other integrable PDEs which admit Lax pairs, such as the nonlinear Schrödinger equation, the sine-Gordon equation or the Kadomtsev-Petviashvili equation. The latter could be particularly insightful since it describes two-dimensional wave fields, a significant increase in complexity over the one-dimensional PDEs which have been studied heretofore.

ACKNOWLEDGEMENTS

This work started life at the Geophysical Fluid Dynamics summer school at Woods Hole Oceanographic Institution, and section VI represents a small part of the fellow's project of CV. The authors wish to thank Peter Schmid for his help with this project, and everyone at GFD for many fruitful discussions. JPP would like to thank Al Osborne for some useful pointers.

AUTHOR DECLARATIONS

The authors have no conflicts to disclose.

DATA AVAILABILITY

The data that supports the findings of this study are available within the supplementary material.

APPENDIX

Here we give a brief overview of the procedure to recover the parameters for the Riemann theta function, i.e. \mathbf{U} , \mathbf{W} and \mathbf{B} , from a time-series of ϑ .

Again assuming $g = 2$, we determine \mathbf{W}_j from ϑ as we did with u . The wavenumber vector \mathbf{U}_j is recovered using the same idea; as each DMD frequency ω_k is an integer linear combination of $i\mathbf{W}_j$, we expect that each DMD spatial mode \mathbf{u}_k will be a pure sinusoid with wavenumber ℓ_j satisfying $i\ell_j = n_{1k}\mathbf{U}_1 + n_{2k}\mathbf{U}_2$. To solve for entries of the period matrix \mathbf{B} , we will need 3 DMD modes, where we can infer n_{1k}, n_{2k} for each mode k . We construct an invertible matrix \mathbf{M} where each row \mathbf{M}_k has entries $(n_{1k}^2, 2n_{1k}n_{2k}, n_{2k}^2)$. Then letting \mathbf{c} be a vector such that $c_k = 2\log(a_k)$, we solve

$$\mathbf{M}\mathbf{b} = \mathbf{c}, \quad \mathbf{b} = (\mathbf{B}_{11}, \mathbf{B}_{21}, \mathbf{B}_{22}) \quad (31)$$

for \mathbf{B} . We note that for $g > 2$, we can still determine all parameters of the Riemann theta function give enough well-resolved DMD nodes. However, given that the symmetric $g \times g$ matrix \mathbf{B} will have $(g+1)g/2$ unique entries, we will need to identify the same number of well-resolved DMD modes which can be a nontrivial task even for small g .

We apply our DMD analysis to KdV data with initial condition $u_0(x) = \sin x$, where we analyze the value of ϑ , rather than u . To three decimal places, we recover the same values for the frequencies (29). Figure 7 shows the eigenvalues, along with the three modes corresponding to frequencies $\tilde{\mathbf{W}}_1$, $\tilde{\mathbf{W}}_2$, and $\tilde{\mathbf{W}}_1 + \tilde{\mathbf{W}}_2$ which were used to determine $\tilde{\mathbf{B}}$. The DMD spectrum for ϑ is much cleaner than for u , which shows that the Hirota transform has in some sense simplified the dynamics.

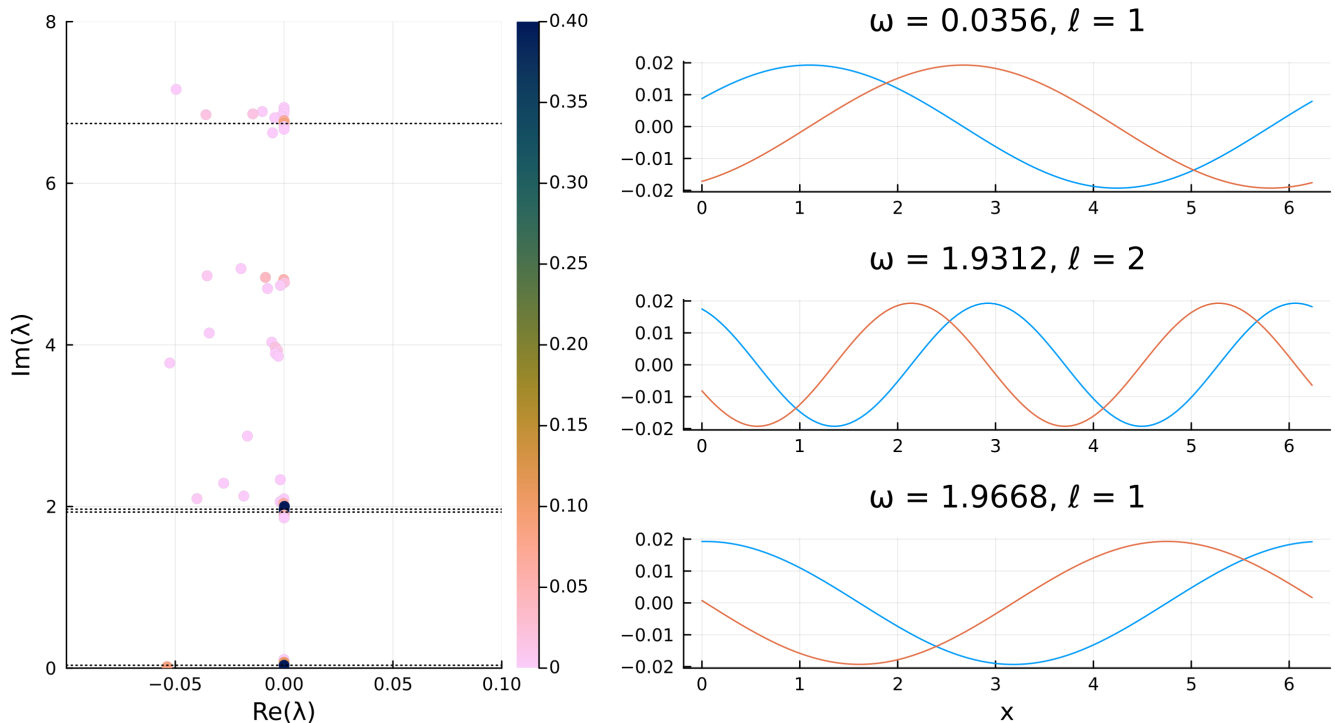


FIG. 7. Left: As for 6 except that data analyzed was of ϑ rather than u . Horizontal lines show ω_j for the well-resolved modes: $\bar{\mathbf{W}}_1 = 0.0356i$, $\bar{\mathbf{W}}_2 = 1.9312i$, $\bar{\mathbf{W}}_1 + \bar{\mathbf{W}}_2 = 1.9668i$, and $\bar{\mathbf{W}}_3 = 6.7394i$. Right: DMD spatial modes corresponding to the given frequencies. The real part of the mode is shown in blue, the imaginary part in orange. For each pattern, we also compute the wavenumber ℓ .

- ¹Bernard O Koopman. Hamiltonian systems and transformation in hilbert space. *Proceedings of the National Academy of Sciences*, 17(5):315–318, 1931.
- ²I. Mezić. Spectral properties of dynamical systems, model reduction and decompositions. *Nonlinear Dynam.*, 41:309–325, 2005. doi:10.1007/s11071-005-2824-x.
- ³I. Mezić. Analysis of fluid flows via spectral properties of the Koopman operator. *Ann. Rev. Fluid Mech.*, 45:357–378, 2013. doi:10.1146/annurev-fluid-011212-140652.
- ⁴P. J. Schmid. Dynamic mode decomposition of numerical and experimental data. *J. Fluid Mech.*, 656:5–28, 2010. doi:10.1017/S0022112010001217.
- ⁵Peter J Schmid, Larry Li, Matthew P Juniper, and O Pust. Applications of the dynamic mode decomposition. *Theoretical and Computational Fluid Dynamics*, 25(1):249–259, 2011.
- ⁶J Nathan Kutz, Steven L Brunton, Bingni W Brunton, and Joshua L Proctor. *Dynamic mode decomposition: data-driven modeling of complex systems*. SIAM, 2016.
- ⁷Peter J. Schmid. Dynamic Mode Decomposition and Its Variants. *Annual Review of Fluid Mechanics*, 54(1):225–254, 2022. doi:10.1146/annurev-fluid-030121-015835. URL <https://doi.org/10.1146/annurev-fluid-030121-015835>.
- ⁸C. W. Rowley, I. Mezić, S. Bagheri, P. Schlatter, and D. S. Henningson. Spectral analysis of nonlinear flows. *J. Fluid Mech.*, 641:115–127, 2009. doi:10.1017/S0022112009992059.
- ⁹J Nathan Kutz, Joshua L Proctor, and Steven L Brunton. Applied Koopman theory for partial differential equations and data-driven modeling of spatio-temporal systems. *Complexity*, 2018, 2018.
- ¹⁰Jacob Page and Rich R Kerswell. Koopman analysis of Burgers equation. *Physical Review Fluids*, 3(7):071901, 2018.
- ¹¹Mikhael Balabane, Miguel Alfonso Mendez, and Sara Najem. Koopman operator for Burgers’s equation. *Physical Review Fluids*, 6(6):064401, 2021.
- ¹²Hiroya Nakao and Igor Mezić. Spectral analysis of the koopman operator for partial differential equations. *Chaos: An Interdisciplinary Journal of Nonlinear Science*, 30(11):113131, 2020.
- ¹³Jeremy P Parker and Jacob Page. Koopman analysis of isolated fronts and solitons. *SIAM Journal on Applied Dynamical Systems*, 19(4):2803–2828, 2020.
- ¹⁴Norman J Zabusky and Martin D Kruskal. Interaction of “solitons” in a collisionless plasma and the recurrence of initial states. *Physical Review Letters*, 15(6):240, 1965.
- ¹⁵Enrico Fermi, P Pasta, Stanislaw Ulam, and Mary Tsingou. Studies of the nonlinear problems. Technical report, Los Alamos National Lab.(LANL), Los Alamos, NM (United States), 1955.
- ¹⁶Peter D Lax. Almost periodic solutions of the KdV equation. *SIAM review*, 18(3):351–375, 1976.
- ¹⁷Eugene D Belokolos, Alexander I Bobenko, Viktor Z Enolskii, Alexander R Its, and Vladimir B Matveev. *Algebro-geometric approach to nonlinear integrable equations*, volume 550. Springer, 1994.
- ¹⁸Diederik Johannes Korteweg and Gustav de Vries. Xli. on the change of form of long waves advancing in a rectangular canal, and on a new type of long stationary waves. *The London, Edinburgh, and Dublin Philosophical Magazine and Journal of Science*, 39(240):422–443, 1895.
- ¹⁹Clifford S Gardner, John M Greene, Martin D Kruskal, and Robert M Miura. Method for solving the korteweg-devries equation. *Physical Review Letters*, 19(19):1095, 1967.
- ²⁰D. J. Benney. Long non-linear waves in fluid flows. *Journal of Mathematics and Physics*, 45(1-4):52–63, 1966. doi:<https://doi.org/10.1002/sapm196645152>. URL <https://onlinelibrary.wiley.com/doi/abs/10.1002/sapm196645152>.
- ²¹D Howell Peregrine. Calculations of the development of an undular bore. *Journal of Fluid Mechanics*, 25(2):321–330, 1966.

- ²²Vladimir Iosifovich Karpman. *Non-linear waves in dispersive media: International series of monographs in natural philosophy*, volume 71. Elsevier, 1975.
- ²³T. Kappeler and P. Topalov. Global wellposedness of KdV in $H^{-1}(\mathbb{T}, \mathbb{R})$. *Duke Mathematical Journal*, 135(2):327–360, 2006. doi:10.1215/S0012-7094-06-13524-X. URL <https://doi.org/10.1215/S0012-7094-06-13524-X>.
- ²⁴Ivan C Christov. Hidden solitons in the Zabusky–Kruskal experiment: Analysis using the periodic, inverse scattering transform. *Mathematics and Computers in Simulation*, 82(6):1069–1078, 2012.
- ²⁵Ryogo Hirota. *The direct method in soliton theory*. Number 155. Cambridge University Press, 2004.
- ²⁶S Novikov, Sergei V Manakov, Lev Petrovich Pitaevskii, and Vladimir Evgeneviĉ Zakharov. *Theory of solitons: the inverse scattering method*. Springer Science & Business Media, 1984.
- ²⁷Alfred Osborne. *Nonlinear Ocean Waves and the Inverse Scattering Transform*. Academic Press, 2010.
- ²⁸Peter D Lax. Integrals of nonlinear equations of evolution and solitary waves. *Communications on pure and applied mathematics*, 21(5):467–490, 1968.
- ²⁹Wilhelm Magnus and Stanley Winkler. *Hill's equation*. Courier Corporation, 2013.
- ³⁰Peter J Baddoo, Benjamin Herrmann, Beverley J McKeon, J Nathan Kutz, and Steven L Brunton. Physics-informed dynamic mode decomposition (pidmd). *arXiv preprint arXiv:2112.04307*, 2021.